ORIGINAL PAPER

Swelling and drug delivery kinetics of click-synthesized hydrogels based on various combinations of PEG and star-shaped PCL: influence of network parameters on swelling and release behavior

Mohammad Saidi[1] · Alaleh Dabbaghi[1] · Sohrab Rahmani[1] 📷

Abstract

Polyethylene glycol (PEG)- and polyethylene glycol–polycaprolactone (PEG–PCL)-based hydrogels were synthesized with various compositions of prepolymers by using ROP and click chemistry methods. Relevant prepolymers were characterized by ^{1}H NMR and FTIR spectroscopy. In order to study the influence of network parameters on swelling and release kinetics, experimental data were approximated by several mathematical models including zero order, first order, Higuchi and Korsmeyer–Peppas to determine the kinetics of swelling and diclofenac sodium release from hydrogels. The obtained results showed that the swelling and release data were best fitted to Korsmeyer–Peppas model. The results of the swelling study showed that the swelling properties of the hydrogels varied with the changes in the PEG molecular weights, as well as concentration of PCL. All of the hydrogels showed non-Fickian diffusion, but when PCL concentration increased and PEG molecular weights decreased, the n values were decreased and reached $n = 0.5$ (Fickian diffusion). The kinetics of diclofenac sodium release from hydrogels showed similar behavior so that in F hydrogels with the highest PCL concentration, the release mechanism fully changed from non-Fickian to Fickian diffusion. In other words, with increasing cross-link density and PCL concentration, the swelling degree and flexibility of networks decreased. Therefore, the swelling and release mechanism changed from non-Fickian to Fickian diffusion.

Keywords Amphiphilic hydrogels · Swelling kinetics · Network parameters · Click chemistry · Drug delivery kinetics

✉ Sohrab Rahmani
  rahmani.sohrab@znu.ac.ir

Extended author information available on the last page of the article

Introduction

Hydrogels are three-dimensional polymeric networks that can absorb a large quantity of water and remain mechanically stable without dissolving [1, 2]. In recent years, hydrogels have found widespread applications in wound dressings [3–5], superabsorbent [6, 7], sensor units [8–10], tissue engineering [11–13], self-healing materials [14–16] and drug delivery vectors [17–19]. Swelling and diffusion behaviors of hydrogels are important parameters for their applications in biomedical and pharmaceutical areas. The swelling behavior of polymer networks can be affected by the nature of the polymer and degree of cross-linking. Swelling behavior and its relationship with structural parameters of hydrogels have been studied by many researchers [20, 21]. Tahar Bartil et al. synthesized pH-sensitive hydrogels based on methacrylic derivatives. Their study revealed that the mechanism of water transport through the gels was significantly affected by the pH of the swelling medium and became more relaxation-controlled in a swelling medium of pH 7.0. The swelling and hydrolytic behaviors of hydrogels were dependent on the content of methacrylic acid (MAA) groups [22]. González-Álvarez et al. synthesized polyacrylamide-co-itaconic acid/chitosan-based hydrogels. Their study showed that the swelling properties of the network varied with the changes in the pH in the swelling solution, as well as concentration of chitosan. Also, the ascorbic acid diffusion inside the hydrogel follows a Fickian mechanism [23]. In another interesting work, Chaenyung Cha et al. synthesized poly(*N*-isopropylacrylamide)-based hydrogels using polyethylene glycol cross-linkers with varying chain lengths. Their study revealed that the swelling/deswelling behavior, drug release and lower critical solution temperature (LCST) of PNIPAm–PEG hydrogels can be affected by the concentration and molecular weight of the polyethylene glycol (PEG) cross-linker [24]. Recently, Dibyendu S. Bag et al. synthesized silver nanoparticles-embedded double-network nanocomposite hydrogels of poly(acrylamide-co-2-hydroxyethyl methacrylate) as the second network and polyvinyl alcohol–borax as the first network by in situ reduction of silver nitrate using citric acid. Antibacterial properties, degree of swelling and swelling kinetics of these hydrogels were fully investigated by the authors. The swelling kinetic study revealed that the diffusion of solvent molecules inside both virgin and silver nanoparticles-embedded double-network hydrogels followed the non-Fickian-type behavior. Furthermore, silver nanoparticles-containing hydrogels exhibited a significant amount of antibacterial activity toward gram-positive and gram-negative bacteria [25]. In respect of polymer nature, using of hydrophobic polymers in hydrogel structure can regulate the swelling and consequently the release behavior of hydrophobic and hydrophilic components. Also, incorporation of hydrophobic segments improves mechanical properties of hydrogels that these materials are defined as amphiphilic polymer co-networks that have found versatile application such as contact lenses [26–28], drug delivery matrices [29, 30], membranes [31] and tissue engineering scaffolds [32, 33]. Swelling and release behaviors of amphiphilic hydrogels have been studied by many researchers [34, 35]. For example, Yang et al. synthesized amphiphilic hydrogels based on

well-defined star-shaped hydrophobic poly(caprolactone) (PCL) and hydrophilic polyethylene glycol (PEG) using ring-opening polymerization and click chemistry. Their studies revealed that the swelling and release behaviors, thermal property and good protein absorption resistance property of the amphiphilic hydrogels are closely related to the composition of hydrophilic and hydrophobic segments [36]. In another work, Chunju He et al. synthesized novel core-first star polymer-based co-networks via sequential atom transfer radical polymerization (ATRP). Their study revealed that synthesized amphiphilic co-networks (APCNs) show a unique swelling behavior and excellent mechanical properties and the release rate could be regulated by varying the hydrophilic composition and cross-linking density [37]. It seems that the network permeability and swelling behavior can be the two most important characteristics of hydrogels in controlled release applications. Therefore, knowledge of the swelling kinetics and network permeability of hydrogels can be important in biomedical and pharmaceutical applications. In the previous work, we synthesized multi-component amphiphilic co-networks based on PCL and PEG prepolymers that the swelling and release rate of these amphiphilic hydrogels could be regulated by establishment of a balance between hydrophilic/hydrophobic compositions and the cross-linking density [38]. In continuation of our previous report, in order to obtain complete information with more details in respect of swelling and release kinetics, in this study pure PEG- and PEG–PCL-based hydrogels were synthesized through ring-opening polymerization and click chemistry methods and the influence of network parameters on swelling and drug release kinetics was investigated.

Experimental

Materials

Polyethylene glycol (PEG, $M_n = 2000$, 4000 and 6000 g/mol) was kindly provided by Kimiagaran Emrooz Chemical Industries Co. and dried by azeotropic distillation in the presence of toluene. Propargyl bromide (80% in toluene) was purchased from Acros Chemical Co. and used as received without further purification. ε-Caprolactone (98%), pentaerythritol, $Sn(Oct)_2$, 4-toluenesulfonyl chloride, sodium azide, sodium ascorbate and copper(II) sulfate pentahydrate were purchased from Merck Chemical Co. and were used as received. Diclofenac sodium was supplied by Alborz Darou. Diethyl ether and THF were dried and distilled from benzophenone–Na. Dimethylformamide (DMF), dichloromethane (DCM) and dimethyl sulfoxide (DMSO) were dried by distillation under reduced pressure over CaH_2 and then stored over molecular sieve 4A. All other chemicals were of analytical grade and were used as received.

Experimental procedure

Synthesis of four-arm star-shaped polycaprolactone (4sPCL)

Under nitrogen atmosphere, 2.28 g ε-CL (20 mmol), pentaerythritol (0.14 g, 1 mmol) and Sn(Oct)$_2$ (0.1 wt% of ε-CL) were added to a three-neck round-bottom flask equipped with a reflux condenser. The reaction mixture was stirred at 130 °C for 48 h. After the reaction flask was cooled down to room temperature, the reaction mixture was dissolved in methylene chloride and then poured into excess diethyl ether to precipitate the polymerized product. The product was obtained after filtering and drying.

Synthesis of tosylated 4sPCL

4sPCL (0.5 g, 0.1 mmol) was dissolved in 20 mL of anhydrous DCM, then triethylamine (0.3 mL, 2 mmol) was added, and the reaction mixture was cooled to 0 °C. A solution of TsCl (0.4 g, 2 mmol) in 5 mL of DCM was slowly added to the reaction mixture. After stirring for 1 h at 0 °C, the reaction was stirred overnight at room temperature. Then, the reaction mixture was filtered and washed three times with distilled water. After drying of organic layer over MgSO$_4$, the tosylated product was obtained after evaporation of excess amount of DCM and precipitation in the excess amount of cold diethyl ether.

Synthesis of azide-functionalized 4sPCL

Sodium azide (0.07 g, 1.06 mmol) was added to a solution of tosylated 4sPCL (0.25 g, 0.05 mmol) in DMF (7 mL). The solution was allowed to stir for 24 h at 45 °C. After reaction completed, insoluble products were filtered. DCM (15 ml) was added to the reaction mixture and washed three times with distilled water. The organic layer was dried over MgSO$_4$, and the product was obtained after evaporation of excess amount of DCM and precipitation in excess amount of cold diethyl ether.

Synthesis of propargylated pentaerythritol

One gram pentaerythritol was dissolved in 15 ml DMSO, and then, 2.5 ml aqueous solution of NaOH (40 wt%) was added. The solution was stirred at room temperature for 30 min. Propargyl bromide (80%, 6 ml) was then added, and the reaction mixture was stirred at room temperature for an additional 10 h. Diethyl ether was added to the reaction mixture and washed three times with distilled water. The organic layer was dried with MgSO$_4$. After evaporation of diethyl ether, yellow viscose crude product was obtained and used without further purification.

Tosylation of polyethylene glycol

Polyethylene glycols ($M_n = 2000$, 4000 and 6000 g/mol) were tosylated according to the following procedure.

Typically, PEG-2000 (3 g, 1.5 mmol) was dissolved in 20 ml dichloromethane and then triethylamine (2.1 ml, 15 mmol) was added. Tosyl chloride (2.86 g, 15 mmol) in 10 ml dichloromethane was added dropwise to this solution at 0 °C. The reaction mixture was stirred at room temperature for 24 h. In continue, the reaction mixture was washed with brine and cold water three times. Organic phase was dried over $MgSO_4$, concentrated under reduced pressure and precipitated in diethyl ether as a white solid. The same procedure was used for tosylation of PEG-4000 and 6000.

Azide-functionalized polyethylene glycol

Typically, tosylated polyethylene glycol (PEG-2000-OTS, 1 g, 0.43 mmol) was dissolved in DMF (10 mL) and sodium azide (0.6 g, 10.7 mmol) was added. The reaction mixture was stirred for 24 h at 70 °C. Dichloromethane (20 mL) was added and the reaction mixture was washed three times with cold distilled water. The organic layer was dried with anhydrous magnesium sulfate. After solvent evaporation, the product was precipitated in diethyl ether as a white solid. The same procedure was used for the synthesis of PEG-4000-$(N_3)_2$ and PEG-6000-$(N_3)_2$.

Preparation of PEG- and PEG–PCL-based hydrogels

Hydrogels have been synthesized by using various combinations of prepolymers as given in Table 1. A 1:1 molar ratio between the azide and alkyne groups was used for all of the hydrogels.

PEG-based hydrogels Typically, in a small vial, PEG-bis-azide (0.1 g, 0.05 mmol) and tri- and tetrafunctional pentaerythritol (0.004 g, 0.032 mmol) were dissolved in a solution of ethanol/isopropanol (1:1 volume ratio, 0.5 mL). Sodium ascorbate (5 mg, 0.025 mmol) in 0.25 mL water was added to this solution, and the mixture was shaken vigorously until a clear solution was obtained. Copper sulfate (5 mg, 0.02 mmol) in 0.25 mL water was added to the solution, and the mixture

Table 1 Compositions of different hydrogels

Hydrogels	Prepolymers				
	PEG-2000-$(N_3)_2$	PEG-4000-$(N_3)_2$	PEG-6000-$(N_3)_2$	Propargylated pentaerythritol	4sPCL-$(N_3)_4$
A	✓			✓	
B		✓		✓	
C			✓	✓	
D	✓ (75%)			✓	✓ (25%)
E	✓ (50%)			✓	✓ (50%)
F	✓ (25%)			✓	✓ (75%)
G				✓	✓

was shaken for 10 s. The hydrogels began to form immediately after the addition of copper (II) sulfate. The reaction was allowed to react at room temperature for another 2 h to obtain a uniform solid structure. After complete gelation, the gel was immersed into firstly ethylenediaminetetraacetic acid (EDTA) solution (5%) and then ethanol to remove copper ions and unreacted precursors. At last, the gel was immersed in deionized water to achieve further purification. The gel fraction was calculated as the weight percentage of dry gel over the total weight of the polymer precursors.

PEG–PCL-based hydrogels Typically, the synthesis procedure for E hydrogel is as follows: PEG diazide (0.03 g, 0.01 mmol), azide-functionalized 4sPCL (0.023 g, 0.005 mmol) and propargylated pentaerythritol (0.0019 g, 0.01 mmol) were dissolved in 0.25 mL DCM in a 5-mL vial. Then, DMF (0.5 mL) was added to the vial. Sodium ascorbate (5 mg, 0.025 mmol) and copper sulfate (3 mg, 0.012 mmol) were dissolved in 0.25 mL water separately, and then, the mixture was added into the vial. The solution was shaken vigorously for 10 s. After 1 h, the hydrogel was formed. The gel was then washed with EDTA solution (5 wt%), DCM and deionized water, respectively, to remove copper ions and unreacted residue.

Characterization

^{1}H NMR spectra were recorded on a Bruker Advance DPX instrument at 250 MHz using CDCl3 as the solvent. Infrared spectra were obtained on a Thermo Scientific Nicolet iS10 FTIR spectrophotometer. The samples were pressed into potassium bromide (KBr) pellets. The morphology of hydrogels was studied on a scanning electron microscope (SEM). The hydrogels were swelled in water for 48 h, then removed from solvent, quickly frozen in liquid nitrogen and then freeze-dried in a Christ alpha 1-4 LD plus freeze drier under vacuum at −60 °C for 3 days until the samples became completely dry. The freeze-dried hydrogels were coated with gold and then visualized using a Seron Technologies ALS2100 SEM. All UV–VIS data are collected with a Heylos spectrophotometer. Diclofenac sodium concentration was determined by measuring the absorbance of the solutions at $\lambda_{max} = 276$ nm.

Swelling measurements

After purification of hydrogels, they were dried at 50 °C under reduced pressure until they reached constant weight prior to swelling measurements. The swelling of the hydrogels was studied by immersing dry hydrogels in deionized water at room temperature. At certain time intervals, hydrogels were removed, wiped with soft tissue to remove excess surface water, and they were weighed at certain time intervals until the swelling equilibration. The degree of swelling (DS) of hydrogels was determined using the following equation:

$$DS = (W_s - W_d)/W_d$$

where W_s and W_d are the weights of the dry and swollen gel, respectively.

Load and release study of diclofenac sodium

Entrapping method was applied for loading of diclofenac sodium into hydrogels. Briefly, during the hydrogel formation process, in addition to prepolymers, solvent and catalyst, 5 mg of diclofenac sodium was also added to the vial. As hydrogels formed, the drug was entrapped into hydrogels. Drug-containing hydrogels were dried at room temperature for 48 h. Release study of diclofenac sodium was done in phosphate-buffered solution (PBS) at 37 °C. Drug-containing hydrogels were immersed in 50 ml phosphate-buffered solution. In certain time intervals, 3 ml of the solution was removed from the release medium and replaced with 3 ml of fresh phosphate-buffered solution. The concentration of diclofenac sodium was measured by UV–VIS spectroscopy at 276 nm. Each measurement was repeated at least two times, and the average values were plotted.

Results and discussion

### Synthesis of prepolymers and cross-linkers

Prepolymers and cross-linkers were synthesized and characterized according to our previous work [37].

Azide-functionalized four-arm star-shaped polycaprolactone was synthesized in three steps which are presented in Scheme 1.

The FTIR spectrum of four-arm sPCL is shown in Fig. 1a(I). The main absorption bands at 1200 and 1725 cm^{-1} are related to ether and carbonyl bonds, respectively. In addition, the appearance of absorption bands of C–H (2945 cm^{-1}) and OH (3435 cm^{-1}) confirms the ring-opening polymerization of CL by the initiator. The ^{1}H NMR spectrum of four-arm sPCL is shown in Fig. 2a. The main resonance peaks (Ha, Hb, Hc, Hd, He) are attributed to methylene protons of PCL repeating units while the terminal methylene protons (Hf) were observed in 3.65 ppm. The ^{1}H NMR spectrum of tosylated sPCL is shown in Fig. 2b. The characteristic signals related to tosyl groups were appeared at 7.3, 7.8 ppm (aromatic protons) and 2.4 ppm (benzylic protons). Tosylate groups were replaced by azide groups via reaction with NaN$_3$ in dry DMF. This substitution was confirmed by fully disappearance of signals related to tosyl groups and appearance of a new peak at 3.30 ppm that can be attributed to protons of –CH$_2$–N$_3$ group (Fig. 2c). This result was also confirmed by FTIR analyses. The absorption peak of azide groups appeared in 2096 cm^{-1} which indicates successful preparation of azide-functionalized sPCL (Fig. 1a (II)).

^{1}H NMR spectra of tosyl and azide-terminated PEG are shown in Fig. 2e, f, respectively. The appearance of aromatic protons (7.31 and 7.74 ppm) and benzylic protons (2.40 ppm) in the spectrum of tosylated PEG indicates that the esterification

Scheme 1 End azide function-
alization of four-arm star-shaped
polycaprolactone
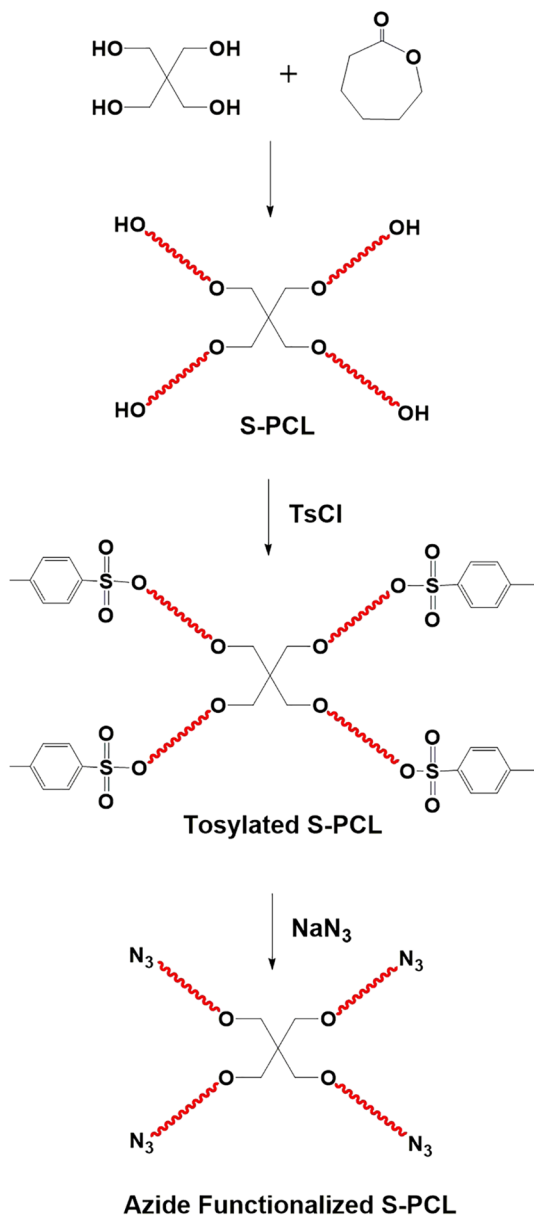
reaction happened successfully. Furthermore, the signals of tosylated PEG at 7.74, 7.31 and 2.3 ppm disappeared fully after reacting with NaN_3 which indicated that sulfonate groups were replaced by azido groups completely.

Figure 2d shows [^1H] NMR spectrum of propargylated pentaerythritol. (Only tri-functional product was shown with spectrum.) With the appearance of peaks at 4.15 ppm ($-OCH_2CCH$), 3.45 ppm ($-CH_2OCH_2CCH$) and 2.35 ppm ($-CCH$) in the
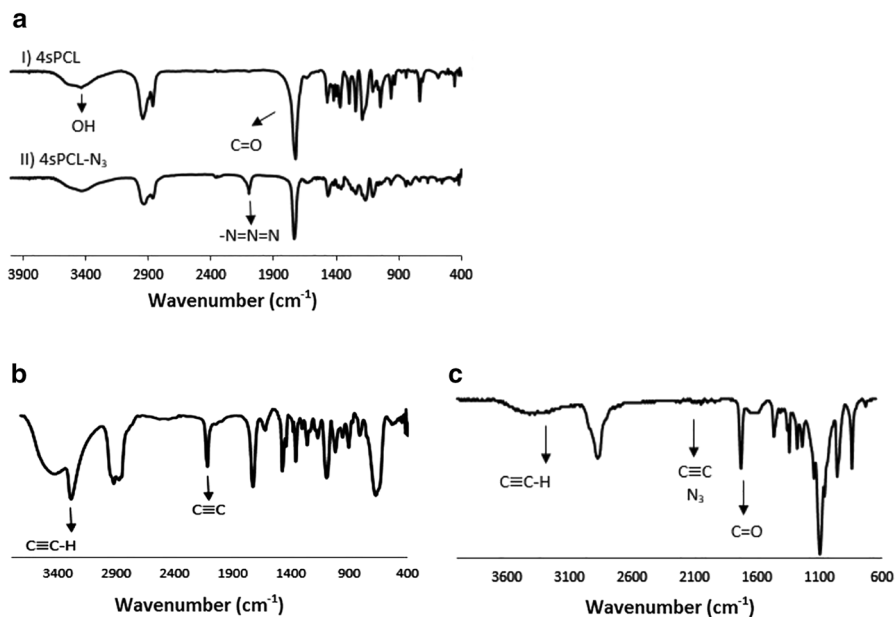
**Fig. 1** FTIR spectra of a (I)) four-arm sPCL, **a** (II)) four-arm sPCL-N$_3$, **b** propargylated pentaerythritol, **c** ATR-FTIR spectrum of PEG–PCL hydrogel

^{1}H NMR spectrum, the functionalization of pentaerythritol with propargyl groups was confirmed. The presence of peak at 3.60 ppm (CH$_2$OH) indicates that the mixture of products (tetra-, tri-, bi- and monofunctional products) was obtained in this reaction. Additionally, the FTIR spectrum is shown in Fig. 1b. The absorption bands at 3290 and 2115 cm^{-1} are attributed to H–C (–C≡C–H) and carbon–carbon triple bond (–C≡C–) stretching vibration, respectively. These results confirm that alkyne functionalization of pentaerythritol was achieved successfully.

Synthesis of PEG- and PEG–PCL-based hydrogels

Seven types of PEG- and PEG–PCL-based hydrogels were synthesized as given in Table 1. All of the hydrogels were synthesized in the presence of CuSO$_4$.5H$_2$O and sodium ascorbate as a click reaction catalyst. In PEG-based hydrogels (A, B and C), the polyethylene glycols with different molecular weights are incorporated in hydrogel networks, while in PEG–PCL-based hydrogels (D, E, F and G), the PEG/PCL ratios are different. It is noticeable that in all of the combinations, the stoichiometric ratio of azide and alkyne is considered. Formation of integrated gels based on PEG and PEG–PCL after click reaction between azide and alkyne groups is shown in Fig. 3a, d, respectively. Dry and swollen states of hydrogels also are presented in these figures.

The proposed click coupling between components of PEG- and PEG–PCL-based hydrogels was presented in Schemes 2 and 3, respectively. Typical FTIR spectrum
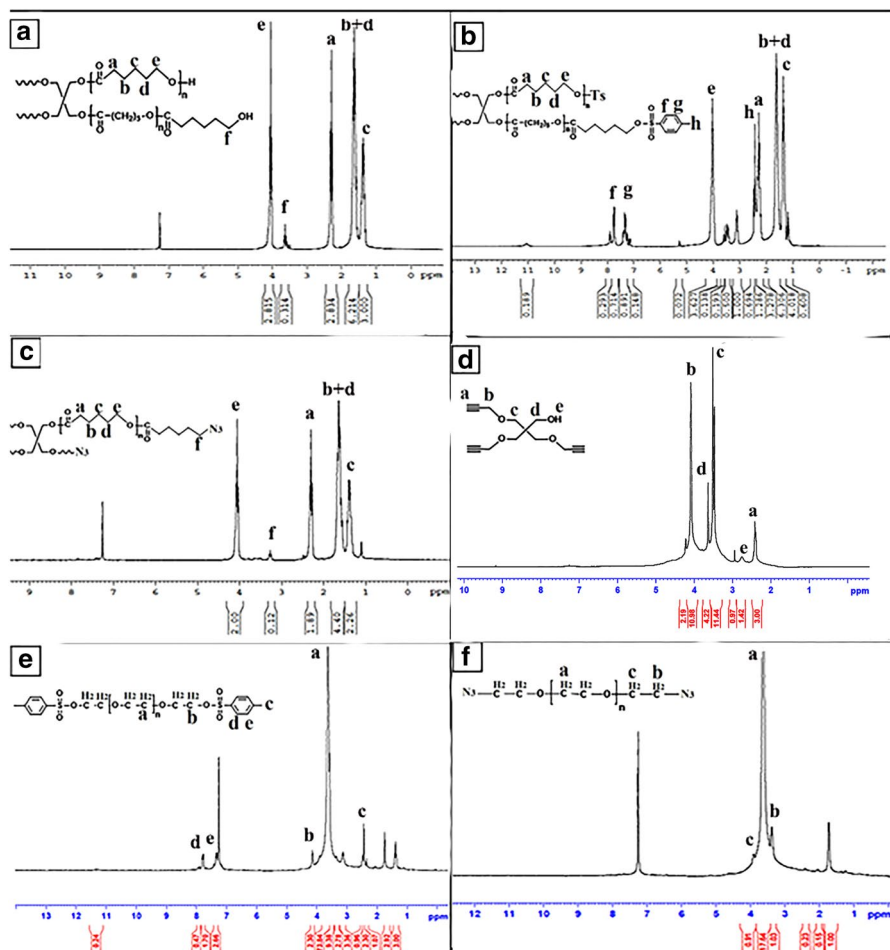
Fig. 2 ^{1}H NMR spectra of **a** 4sPCL, **b** 4sPCL-OTs, **c** 4sPCL-N$_3$, **d** propargylated pentaerythritol, **e** tosyl-terminated PEG, **f** azide-terminated PEG

of PEG–PCL hydrogel is shown in Fig. 1c. The disappearance of the absorbance peak at about 3270 cm^{-1} and 2100 cm^{-1} (related to alkyne groups) and 2096 cm^{-1} (related to azide group) after gelation indicated that the click reaction happened successfully between the azide and alkyne groups.

The morphology of hydrogels was also investigated by scanning electron microscopy (SEM). Figure 4a–d shows the surface and cross-sectional scanning electron microscopy (SEM) images of the typical freeze-dried pure PEG gel. Surface and cross-sectional SEM images of the typical freeze-dried PEG–PCL sample are also shown in Fig. 4e, f, respectively. The morphology of PEG–PCL network is similar to that of the PEG-based network, while the pure PEG gel shows highly porous structure with larger pore sizes. Incorporation of the PCL segments in network leads to a denser morphology of PEG–PCL-based hydrogels (Fig. 4f).
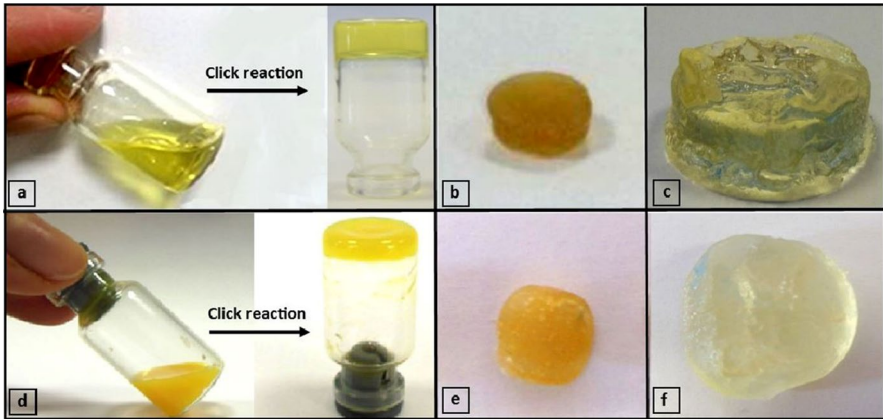
Fig. 3 **a** Formation of pure PEG-based hydrogel by click reaction, **b** hydrogel in dry state, **c** swollen in water, **d** formation of PEG–PCL-based hydrogel by click reaction, **e** hydrogel in dry state, **f** swollen in water
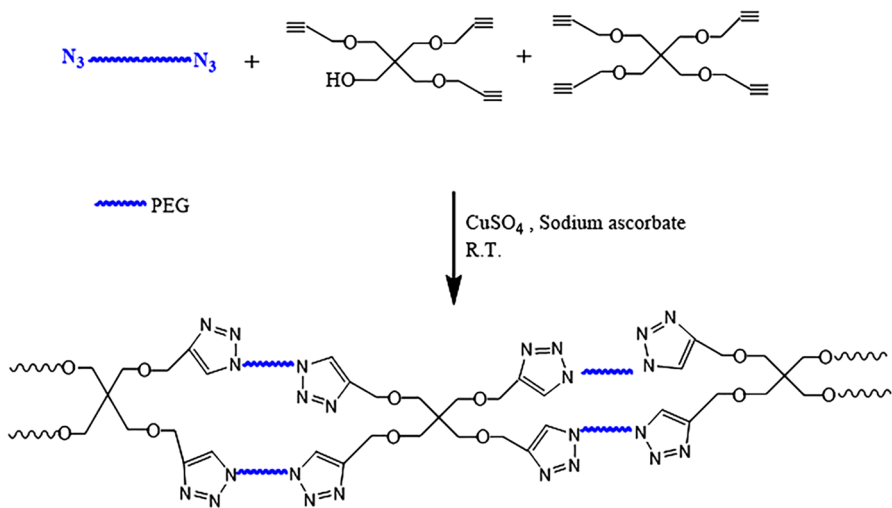
Scheme 2 Click coupling between azide and alkyne groups in pure PEG hydrogels

Swelling behavior

The swelling behavior of pure PEG hydrogels is shown in Fig. 5. It can be clearly seen that the swelling degree of hydrogels was increased with increasing PEG molecular weight but the time taken to achieve equilibrium swelling was decreased. It can be attributed to the cross-link density. In the case of PEG-2000 (A hydrogel), cross-link density in network is higher than in PEG-4000 (B hydrogel) and PEG-6000 (C hydrogel). Therefore, the time reaching equilibrium swelling in A hydrogel is longer than in B and C hydrogels. Figure 6 shows the
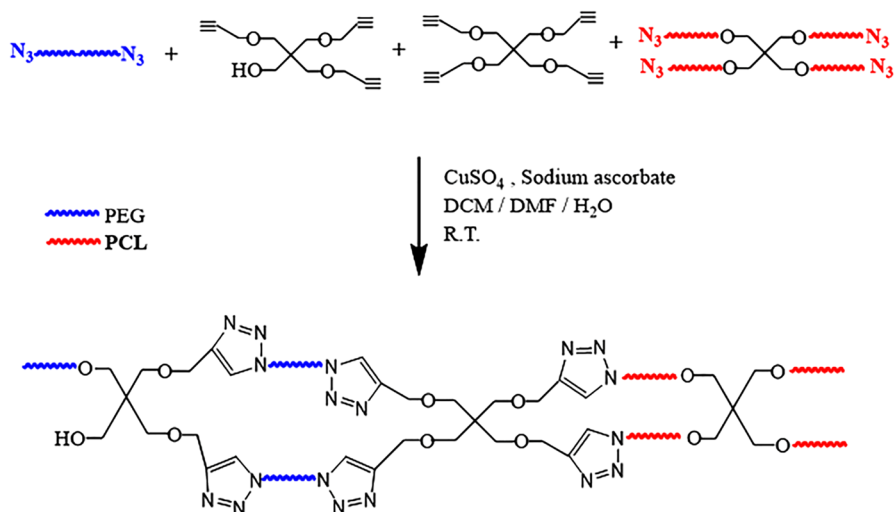
Scheme 3 Click coupling between azide and alkyne groups in PEG–PCL hydrogels

swelling curves of PEG–PCL hydrogels. As shown in Fig. 6, swelling degree of these hydrogels is lower than that of pure PEG hydrogels. These results are expected because with incorporation of PCL segments, the hydrophilicity of networks was decreased. When the contribution of PCL segments was increased in networks (from D to F hydrogels), the swelling degree was decreased in which the G hydrogel does not swell in water. The numerical values of equilibrium swelling of the hydrogels are presented in Table 2. As given in Table 2, the degree of equilibrium swelling was decreased from A to F hydrogels.

Kinetic swelling studies were investigated to explain the mechanism of water diffusion into the hydrogel samples. According to the good adaptation of swelling data with Korsmeyer–Peppas model, Eq. (1) was used to process the kinetic data of the swelling process, in order to obtain information related to the mechanism of water transport through the hydrogels.

$$M_t/M_\infty = kt^n \tag{1}$$

where M_t is the mass of water absorbed at time t, M_∞ is the mass of water absorbed at equilibrium, k (min^{-n}) is the kinetic constant of the hydrogel and n is the swelling exponent describing the mechanism of transport. Fickian diffusion and Case II (relaxation-controlled) transport are defined by n values of 0.5 and 1, respectively. Non-Fickian or anomalous transport is between Fickian and Case II ($0.5 < n < 1$).

The portion of the water absorption curve with fractional water uptake (M_t/M_∞) less than 0.60 was analyzed using Eq. (1). The constants n and k were calculated from the slopes and intercepts of the plots of ln (M_t/M_∞) versus ln t from the experimental data. The graphs of ln (M_t/M_∞) versus ln t for swelling behavior of hydrogels are presented in Fig. 7. According to these graphs, there is a good adaptation of swelling data with Korsmeyer–Peppas model.
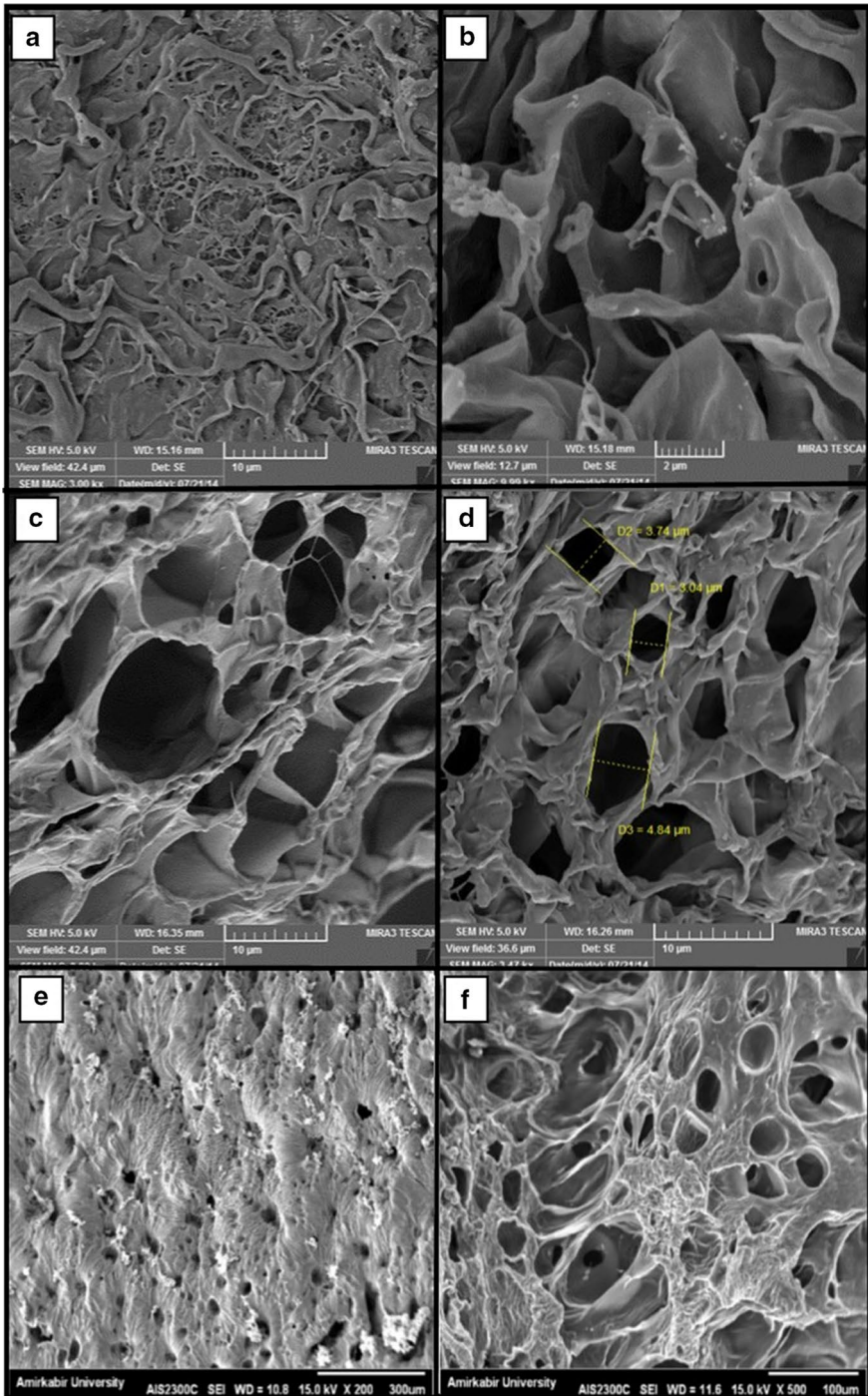
Fig. 4 a SEM of pure PEG-based hydrogel surface, **b**, **c**, **d** SEM of pure PEG-based hydrogel cross section, **e** SEM of PEG–PCL-based hydrogel surface, **f** SEM of PEG–PCL-based hydrogel cross section
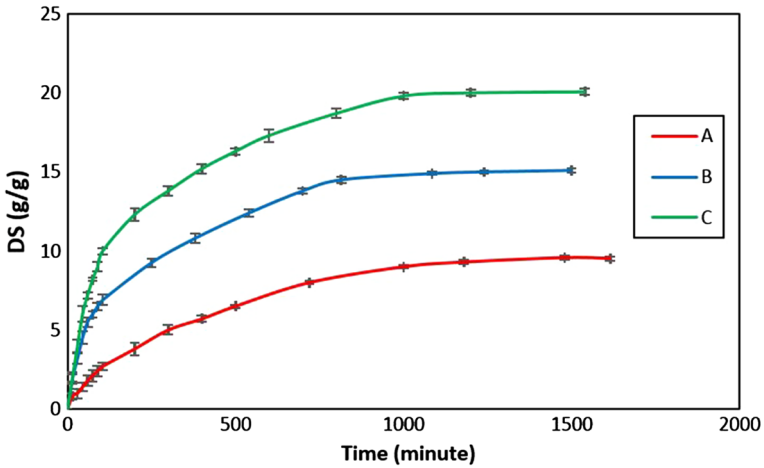
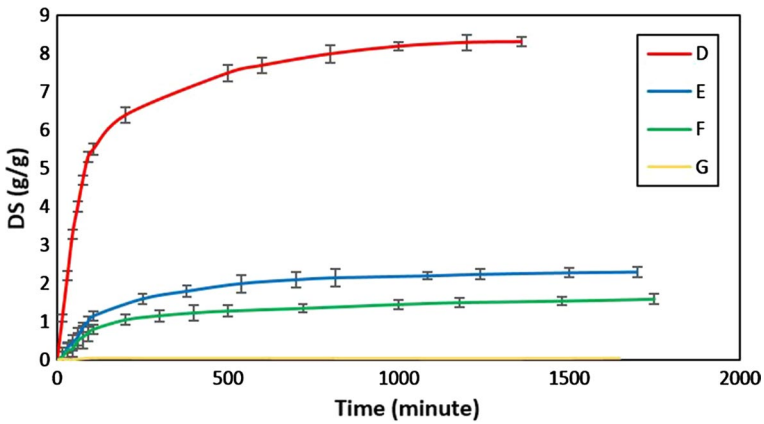**Fig. 5** Swelling degree of A, B and C hydrogels in water

Fig. 6 Swelling degree of D, E, F and G hydrogels in water

Table 2 Swelling equilibrium and kinetic parameters of swelling with the Korsmeyer–Peppas model

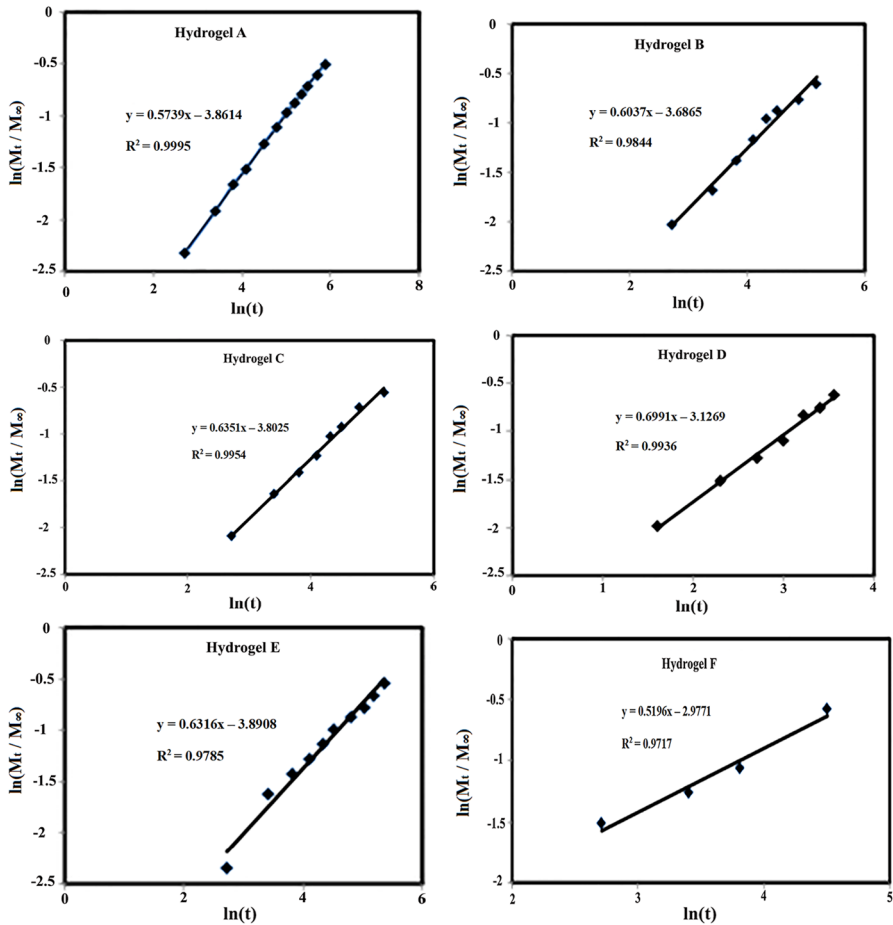| Hydrogels	Swelling equilibrium	R^2	k	n	Swelling mechanism
A	20	0.9995	0.0210	0.5739	Anomalous (non-Fickian)
B	14.5	0.9844	0.0250	0.6087	Anomalous (non-Fickian)
C	9	0.9954	0.0223	0.6351	Anomalous (non-Fickian)
D	8	0.9936	0.0438	0.6991	Anomalous (non-Fickian)
E	2	0.9785	0.0204	0.6316	Anomalous (non-Fickian)
F	1.5	0.9717	0.0509	0.5196	Anomalous (non-Fickian)

Fig. 7 Swelling kinetic plots [ln (M_t/M_∞) versus ln t] of the hydrogels

It is well known that swelling property is related to the structural parameters of the cross-linked polymers.

Table 2 shows swelling mechanism and related kinetic data for various hydrogels. According to the diffusion exponent parameter (n) values, the diffusion of water was found to be anomalous (non-Fickian) for PEG and PEG–PCL hydrogels. The dynamic swelling behavior of cross-linked polymers is dependent on the relative contribution of penetrant diffusion and polymer relaxation. As given in Table 2, for pure PEG hydrogels, the n values were decreased from C to A hydrogel and these values approach to Fickian (diffusion-controlled) behavior. The similar behavior was observed for PEG–PCL hydrogels when the contribution of PCL segments was increased in networks (from D to F hydrogel). It can be attributed to the flexibility of the networks. When a dry hydrogel is placed in water, the polymer chains interact with the solvent molecules, leading to chain expansion, which,

in turn, affects macromolecular chain relaxation. As a result, the extent of separation between the polymer chains depends on the rate of water diffusion into the network. In PEG–PCL hydrogels, with increasing PCL segments, the hydrophobicity of networks is increased. Therefore, the swelling and expansion of polymer chains are restricted and the structure of networks could be more rigid or less flexible. Consequently, with increasing PCL segments in PEG–PCL hydrogels, the mechanism of water transport in the hydrogels changes from non-Fickian to Fickian behavior. This behavior also was observed in pure PEG hydrogels. With decreasing molecular weight of PEG, the cross-link density was increased and consequently the flexibility of networks was decreased.

Drug release studies

The capability of hydrogels as drug carriers was evaluated by determination of their release behavior in phosphate-buffered solution (PBS) at 37 °C. Diclofenac sodium was our model compound to study the release characteristics of water-soluble drugs. The release behavior of diclofenac sodium from A, B and C hydrogels is shown in Fig. 8. As shown in Fig. 8, the rate of release increases as the molecular weight of PEG increases and the release time decreases inversely. With increasing cross-link density, the swelling of networks decreases so the release rate is also reduced. Figure 9 shows the release profiles of PEG–PCL (D, E and F) hydrogels. As shown in Fig. 9, D hydrogel released about 78% of diclofenac sodium within 57 h, while E and F hydrogels released only about 38% and 14% of diclofenac sodium, respectively, at the same time. It seems that the rate of release could be affected by the relative hydrophobic/hydrophilic composition and cross-link density. It can be attributed to PCL amount in D, E and F hydrogels. Drug release is slowest when the hydrophobic content is highest (75 wt%) in the F hydrogel. In other words, the rate of release increases as the amount of the hydrophilic component increases. The release times
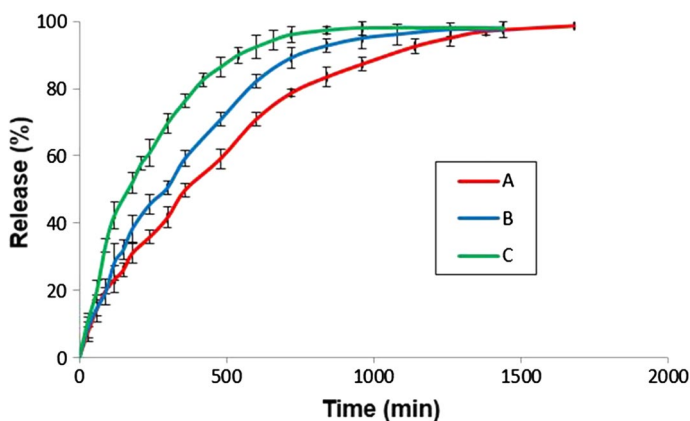
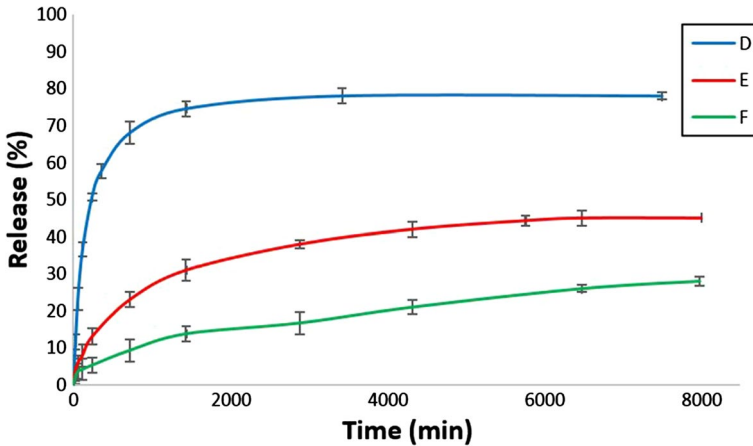**Fig. 8** Release profiles of diclofenac sodium from A, B and C hydrogels

Fig. 9 Release profiles of diclofenac sodium from D, E and F hydrogels

of PEG–PCL hydrogel are longer than those of pure PEG hydrogels, because of the combined effects of increasing PCL contents and cross-link densities.

Drug release kinetics

In order to determine the kinetics of diclofenac sodium release from the hydrogels, various kinetic models were used to analyze release data. Mathematical equations of each model are listed in Table 3. The release data were fitted to kinetic models in order to select the best model based on the correlation coefficient (R^2). Table 4 shows the correlation coefficient of each model for diclofenac sodium release from hydrogels. The obtained coefficient correlation values showed the data were best fitted to Korsmeyer–Peppas model for all of the hydrogels. The graphs of ln (M_t/M_∞) versus ln t for release behavior of hydrogels are presented in Fig. 10. According to these graphs, there is a good adaptation of release data with Korsmeyer–Peppas model.

The mechanism of release can be analyzed by the release exponent n. In Fickian diffusion ($n = 0.5$), the diffusion of penetrant is slower than polymer relaxation and transport is controlled by the diffusion rate. When $n = 1$, polymer relaxation is slower than the diffusion and transport is controlled by the rate of polymer relaxation (Case II transport). The rates of polymer relaxation and diffusion are comparable for non-Fickian diffusion ($0.5 < n < 1$). According

Table 3 Mathematical representations of models used to describe the release profile of diclofenac sodium	Model	Mathematical equation
	Zero order	$Q_t = K_0\,t + Q_0$
	First order	Ln $Q_t =$ Ln $Q_0 + K_1\,t$
	Korsmeyer–Peppas	Ln $(M_t/M_\infty) =$ Ln $K + n$ Ln t
	Higuchi	$Q_t = K_H\,t^{1/2}$

Table 4 Kinetic parameters and release mechanism of diclofenac sodium

Hydrogels	Zero order		First order		Higuchi		Korsmeyer–Peppas			Mechanism
	K	R^2	K	R^2	K	R^2	K	R^2	n	
A	0.0591	0.8985	0.0011	0.7176	2.871	0.9779	0.0075	0.9935	0.7113	Anomalous (non-Fickian)
B	0.0757	0.8901	0.0016	0.7059	3.299	0.9724	0.0061	0.9919	0.7781	Anomalous (non-Fickian)
C	0.0902	0.8255	0.0016	0.6249	3.580	0.9426	0.0061	0.9820	0.8673	Anomalous (non-Fickian)
D	0.0151	0.5214	0.0002	0.3582	1.168	0.7448	0.0093	0.9854	0.8263	Anomalous (non-Fickian)
E	0.0061	0.8350	0.0002	0.6541	0.5619	0.9574	0.0135	0.9964	0.5517	Anomalous (non-Fickian)
F	0.0032	0.9391	0.0002	0.7509	0.3063	0.9868	0.0194	0.9899	0.4430	Fickian
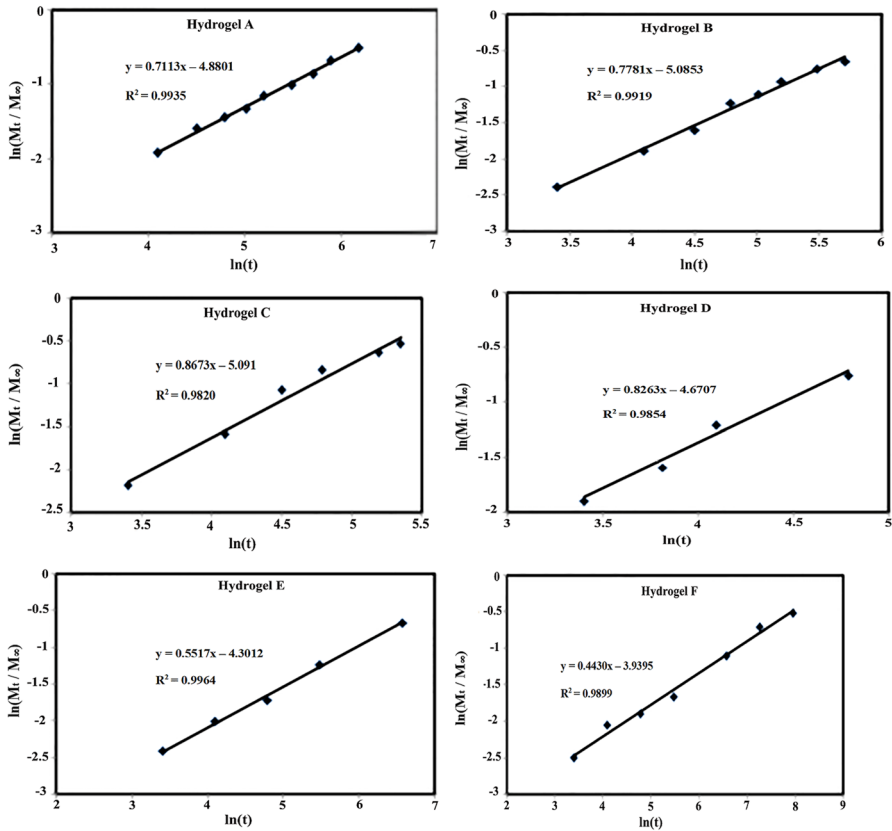
Fig. 10 Release kinetic plots of diclofenac sodium [ln (M_t/M_∞) versus ln t] from hydrogels

to n values presented in Table 4, pure PEG hydrogels show non-Fickian diffusion; however, with decreasing PEG molecular weight, n values were decreased. Interestingly, in the case of PEG–PCL hydrogels, with increasing PCL content, the n values decrease from D to F hydrogel so that in F hydrogel it reaches 0.44. It seems that the polymer relaxation is significantly affected by flexibility of the networks. In PEG–PCL hydrogels, due to incorporation of hydrophobic PCL segments and increasing cross-link density, the flexibility of networks was decreased. Therefore, the rate of polymer relaxation overcomes to rate of penetrant diffusion and release mechanism is controlled through the rate of diffusion. According to n values presented in Table 4, the release mechanism changes from non-Fickian to Fickian diffusion in F hydrogel. In pure PEG hydrogels, with decreasing PEG molecular weight, the flexibility of networks was decreased and the n values were decreased. These results have good adaptation with swelling results (Table 2).

Conclusion

In this study, pure PEG- and PEG–PCL-based hydrogels have been synthesized through a combination of ROP and click chemistry in order to determine the influence of structural parameter on their swelling kinetic and diclofenac sodium release. It was found that the PEG molecular weight and the relative hydrophobic/hydrophilic composition have a significant effect on swelling and release mechanism. The swelling and release data were best fitted to Korsmeyer–Peppas model. With increasing cross-link density and PCL concentration, the swelling degree and flexibility of networks decrease. Therefore, the swelling and release mechanism changes from non-Fickian to Fickian diffusion.

References

1. Ahmed EM (2015) Hydrogel: preparation, characterization, and applications: a review. J Adv Res 6:105–121. https://doi.org/10.1016/j.jare.2013.07.006
2. Sannino A, Demitri C, Madaghiele M (2009) Biodegradable cellulose-based hydrogels: design and applications. Materials 2:353–373. https://doi.org/10.3390/ma2020353
3. Chen T, Chen Y, Rehman HU et al (2018) Ultratough, self-healing, and tissue-adhesive hydrogel for wound dressing. ACS Appl Mater Interfaces 10:33523–33531. https://doi.org/10.1021/acsami.8b10064
4. Chen H, Cheng J, Ran L et al (2018) An injectable self-healing hydrogel with adhesive and antibacterial properties effectively promotes wound healing. Carbohydr Polym 201:522–531. https://doi.org/10.1016/j.carbpol.2018.08.090
5. Qu J, Zhao X, Liang Y, Zhang T, Ma PX, Guo B (2018) Antibacterial adhesive injectable hydrogels with rapid self-healing, extensibility and compressibility as wound dressing for joints skin wound healing. Biomaterials 183:185–199. https://doi.org/10.1016/j.biomaterials.2018.08.044
6. Behrouzi M, Moghadam PN (2018) Synthesis of a new superabsorbent copolymer based on acrylic acid grafted onto carboxymethyl tragacanth. Carbohydr Polym 202:227–235. https://doi.org/10.1016/j.carbpol.2018.08.094
7. Wang Z, Ning A, Xie P et al (2017) Synthesis and swelling behaviors of carboxymethyl cellulose-based superabsorbent resin hybridized with graphene oxide. Carbohydr Polym 157:48–56. https://doi.org/10.1016/j.carbpol.2016.09.070
8. Ohm C, Brehmer M, Zentel R (2010) Liquid crystalline elastomers as actuators and sensors. Adv Mater 22:3366–3387. https://doi.org/10.1002/adma.200904059
9. Sun JY, Keplinger C, Whitesides GM, Suo Z (2014) Ionic skin. Adv Mater 26:7608–7614. https://doi.org/10.1002/adma.201403441
10. Massad-Ivanir N, Shtenberg G, Zeidman T, Segal E (2010) Construction and characterization of porous SiO₂/hydrogel hybrids as optical biosensors for rapid detection of bacteria. Adv Funct Mater 20:2269–2277. https://doi.org/10.1002/adfm.201000406
11. Drury JL, Mooney DJ (2003) Hydrogels for tissue engineering: scaffold design variables and applications. Biomaterials 24:4337–4351. https://doi.org/10.1016/S0142-9612(03)00340-5
12. Liu W, Deng C, McLaughlin CR et al (2009) Collagen–phosphorylcholine interpenetrating network hydrogels as corneal substitutes. Biomaterials 30:1551–1559. https://doi.org/10.1016/j.biomaterials.2008.11.022
13. Torres-Rendon JG, Femmer T, De Laporte L et al (2015) Bioactive gyroid scaffolds formed by sacrificial templating of nanocellulose and nanochitin hydrogels as instructive platforms for biomimetic tissue engineering. Adv Mater 27:2989–2995. https://doi.org/10.1002/adma.201405873

14. Jia H, Huang Z, Fei Z, Dyson PJ, Zheng Z, Wang X (2016) Unconventional tough double-network hydrogels with rapid mechanical recovery, self-healing, and self-gluing properties. ACS Appl Mater Interfaces 8:31339–31347. https://doi.org/10.1021/acsami.6b11241

15. Yuan N, Xu L, Wang H et al (2016) Dual physically cross-linked double network hydrogels with high mechanical strength, fatigue resistance, notch-insensitivity, and self-healing properties. ACS Appl Mater Interfaces 8:34034–34044. https://doi.org/10.1021/acsami.6b12243

16. Deng Y, Huang M, Sun D et al (2018) Dual physically cross-linked κ-carrageenan-based double network hydrogels with superior self-healing performance for biomedical application. ACS Appl Mater Interfaces 10:37544–37554. https://doi.org/10.1021/acsami.8b15385

17. Zha L, Banik B, Alexis F (2011) Stimulus responsive nanogels for drug delivery. Soft Matter 7:5908–5916. https://doi.org/10.1039/C0SM01307B

18. Hoare TR, Kohane DS (2016) Hydrogels in drug delivery: progress and challenges. Polymer 49:1993–2007. https://doi.org/10.1016/j.polymer.2008.01.027

19. Li J, Mooney DJ (2006) Designing hydrogels for controlled drug delivery. Nat Rev Mater 1:16071. https://doi.org/10.1038/natrevmats.2016.71

20. Bajpai SK, Singh S (2006) Analysis of swelling behavior of poly (methacrylamide-co-methacrylic acid) hydrogels and effect of synthesis conditions on water uptake. React Funct Polym 66:431–440. https://doi.org/10.1016/j.reactfunctpolym.2005.09.003

21. Singh TRR, McCarron PA, Woolfson AD, Donnelly RF (2009) Investigation of swelling and network parameters of poly (ethylene glycol)-crosslinked poly (methyl vinyl ether-co-maleic acid) hydrogels. Eur Polym J 45:1239–1249. https://doi.org/10.1016/j.eurpolymj.2008.12.019

22. Bartil T, Bounekhel M, Cedric C, Jeerome R (2007) Swelling behavior and release properties of pH-sensitive hydrogels based on methacrylic derivatives. Acta Pharm 57:301–314. https://doi.org/10.2478/v10007-007-0024-6

23. Martinez-Ruvalcaba A, Sanchez-Diaz J, Becerra F, Cruz-Barba L, Gonzalez-Alvarez A (2009) Swelling characterization and drug delivery kinetics of polyacrylamide-co-itaconic acid/chitosan hydrogels. Express Polym Lett 3:25–32. https://doi.org/10.3144/expresspolymlett.2009.5

24. Kim S, Lee K, Cha C (2016) Refined control of thermoresponsive swelling/deswelling and drug release properties of poly (N-isopropylacrylamide) hydrogels using hydrophilic polymer crosslinkers. J Biomater Sci Polym Ed 27:1698–1711. https://doi.org/10.1080/09205063.2016.1230933

25. Dixit A, Kumar N, Bag DS, Agarwal K, Sharma Dhirendra K, Prasad NE (2019) Synthesis of AgNPs embedded double network nanocomposite hydrogels having high swelling and anti-bacterial characteristics. Adv Mater Lett 10:431–439. https://doi.org/10.5185/amlett.2019.2258

26. Xu J, Li X, Sun F (2011) In vitro and in vivo evaluation of ketotifen fumarate-loaded silicone hydrogel contact lenses for ocular drug delivery. Drug Deliv 18:150–158. https://doi.org/10.3109/10717544.2010.522612

27. Nicolson PC, Vogt J (2001) Soft contact lens polymers: an evolution. Biomaterials 22:3273–3283. https://doi.org/10.1016/S0142-9612(01)00165-X

28. Kim J, Conway A, Chauhan A (2008) Extended delivery of ophthalmic drugs by silicone hydrogel contact lenses. Biomaterials 29:2259–2269. https://doi.org/10.1016/j.biomaterials.2008.01.030

29. Lin C, Gitsov I (2010) Preparation and characterization of novel amphiphilic hydrogels with covalently attached drugs and fluorescent markers. Macromolecules 43:10017–10030. https://doi.org/10.1021/ma102044n

30. Gitsov I, Zhu C (2003) Novel functionally grafted pseudo-semi-interpenetrating networks constructed by reactive linear—dendritic copolymers. J Am Chem Soc 125:11228–11234. https://doi.org/10.1021/ja0345625

31. Guzman G, Nugay T, Nugay I, Nugay N, Kennedy J, Cakmak M (2015) High strength bimodal amphiphilic conetworks for immunoisolation membranes: synthesis, characterization, and properties. Macromolecules 48:6251–6262. https://doi.org/10.1021/acs.macromol.5b01343

32. Sun Y, Collett J, Fullwood NJ, Mac Neil S, Rimmer S (2007) Culture of dermal fibroblasts and protein adsorption on block conetworks of poly (butyl methacrylate-block-(2,3 propandiol-1-methacrylate-stat-ethandiol dimethacrylate)). Biomaterials 28:661–670. https://doi.org/10.1016/j.biomaterials.2006.09.024

33. Rimmer S, German MJ, Maughan J et al (2005) Synthesis and properties of amphiphilic networks 3: preparation and characterization of block conetworks of poly (butyl methacrylate-block-(2,3 propandiol-1-methacrylate-stat-ethandiol dimethacrylate)). Biomaterials 26:2219–2230. https://doi.org/10.1016/j.biomaterials.2004.07.013

34. Kurian P, Zschoche S, Kennedy J (2000) Synthesis and characterization of novel amphiphilic block copolymers di-, tri-, multi-, and star blocks of PEG and PIB. J Polym Sci Part A Polym Chem 38:3200–3209. https://doi.org/10.1002/1099-0518
35. Truong V, Blakey I, Whittaker AK (2012) Hydrophilic and amphiphilic polyethylene glycol-based hydrogels with tunable degradability prepared by "click" chemistry. Biomacromolecules 13:4012–4021. https://doi.org/10.1021/bm3012924
36. Wang C-W, Liu C, Zhu X-W et al (2016) Synthesis of well-defined star-shaped poly(ε-caprolactone)/poly (ethylene glycol) amphiphilic co-networks by combination of ring opening polymerization and "click" chemistry. J Polym Sci Part A Polym Chem 54:407–417. https://doi.org/10.1002/pola.27790
37. Wang H, Qin A, Li X, Zhao X, Liu D, He C (2015) Biocompatible amphiphilic conetwork based on crosslinked star copolymers: a potential drug carrier. J Polym Sci Part A Polym Chem 53:2537–2545. https://doi.org/10.1002/pola.27721
38. Dabbaghi A, Rahmani S (2019) Synthesis and characterization of biodegradable multicomponent amphiphilic conetworks with tunable swelling through combination of ring-opening polymerization and "click" chemistry method as a controlled release formulation for 2,4-dichlorophenoxyacetic acid herbicide. Polym Adv Technol 30:368–380. https://doi.org/10.1002/pat.4474

Affiliations

Mohammad Saidi[1] · Alaleh Dabbaghi[1] · Sohrab Rahmani[1]

Mohammad Saidi
mohammad.saidi404@gmail.com

Alaleh Dabbaghi
alalehdabbaghi@yahoo.com

[1]   Laboratory of Polymer Synthesis, Department of Chemistry, Faculty of Science, University of Zanjan, Zanjan, Iran